Electronic Supplementary Material (ESI)
for Chem. Commun.

Synthesis of Single-site Copper Catalysts for Methane Partial Oxidation

Sebastian Grundner, Wanqiu Luo, Maricruz Sanchez-Sanchez and Johannes A. Lercher**

Department of Chemistry and Catalysis Research Center, Technische Universität
München, Lichtenbergstr. 4, D-85747 Garching, Germany

Corresponding authors: m.sanchez@tum.de; johannes.lercher@ch.tum.de; Fax: +49 89 289 13544; Tel.: +49 89 289 13540

Supporting Information

S.1 Experimental section

S.1.1 Catalyst synthesis

The Brønsted acidic form of MOR, H-MOR, was obtained by calcination of a commercial zeolite NH_4-MOR (Clariant, Si/Al = 11) in synthetic air at 500 °C for 8 h. The same batch of the parent material as in our previous work was used. Na-MOR was prepared by exchange of H-MOR with 0.5 M $NaNO_3$ at 60 °C for 24 h. Cu-MOR samples with different Cu/Al ratios were prepared by ion exchange of H-MOR and Na-MOR with Cu^{2+} in aqueous phase at ambient temperature. $Cu(CH_3COO)_2$ H_2O, $Cu(NO_3)$ H_2O as well as $CuCl_2$ were used as Cu precursors. The molarity of these solutions (100 ml g^{-1} zeolite) was varied between 0.01 and 0.001 M. The pH value was adjusted by dropwise addition of HNO_3 (0.01 M) or NH_4OH (10 wt.% in H_2O) respectively. Identical Cu loadings and methane oxidation activities were obtained, if $[N(C_4H_9)_4]OH$ (40% in H_2O) was used for pH adjustment. After the last exchange step, the samples were rinsed four times with deionized water (50 ml g^{-1} MOR each time) with an intermittent centrifugation between each rinse and finally dried at 110 °C for 24 h.

S.1.2 Selective oxidation of methane to methanol

Cu-MOR samples (100 mg) were tested for their activity towards methane oxidation in an atmospheric pressure stainless steel plug flow reactor with 4 mm inner diameter. The reaction included three consecutive steps: (i) activation in O_2 at 450 C for 1h, (ii) CH_4 loading at 200 °C for 4h and (iii) steam-assisted CH_3OH desorption at 135 °C for 30 min, with an intermediate He purge between each step. The reaction products were identified and quantified by online mass spectroscopy (m/z 28, 31, 44 and 46 for CO, CH_3OH, CO_2 and $(CH_3)_2O$, respectively). $(CH_3)_2O$ formed via condensation of two partially oxidized CH_4 molecules corresponds to two CH_3OH equivalents. The sum of all detected products is referred to as total yield or methane converted.

S.1.3 IR spectroscopy

The samples for IR spectroscopy were prepared as self-supporting wafers (10 $mg \cdot cm^{-3}$) and first activated in vacuum ($1.0 \cdot 10^{-7}$ mbar) at 450 °C for 1 h. Infrared spectra of adsorbed n-hexane were recorded at 30 °C on a Vertex 70 spectrometer from Bruker Optics at a resolution of 4 cm^{-1}. Infrared spectra of adsorbed pyridine were measured on a Thermo Nicolet 5700 FT-IR spectrometer with a resolution of 4 cm^{-1}. After activation, subsequent adsorption (30 min) and evacuation of 0.1 mbar pyridine (1 h), the total concentration of Brønsted acid sites (BAS) was determined at 150 °C by integration of the IR band at 1540 cm^{-1}.

S.1.4 NH_3-TPD

Acid sites were further characterized by temperature-programmed desorption of NH_3. After activation at 450 °C 1 mbar NH_3 was adsorbed on the pelletized sample. After equilibration for 3 h and outgassing for 2h, the sample was heated (10 °C min^{-1}) under dynamic vacuum while the NH_3 desorption was monitored by mass spectrometry (m/z 16).

S.2 Back-exchange of active Cu for Na

Cu-MOR samples were first calcined for 2h at 500 °C under O_2 flow. The calcined samples were then exchanged with 0.5 M $NaNO_3$ solution for 24h at 60 °C, and finally rinsed four times with deionized water (50 ml per g MOR each time) with centrifugation between each rinse. These rinse cycles were performed to ensure that the pores did not contain further non-exchanged Na or Cu ions, which would form large CuO clusters during activation. Finally the samples were dried at 110 °C for 24 h.

Following this protocol, active copper oxo clusters are hydrolyzed and back-exchanged into the solution in a quantitative manner, as can be seen by the results from elemental analysis. For all samples prepared below pH 5.7 more than 90% of the Cu was back-exchanged for Na (see Table S2). The total yield of methane oxidation products after back-exchange in the range of 2-6 μmol g^{-1} compared to total yields in the range of 100-150 μmol g^{-1} before back-exchange indicates that more than 95% of the active sites are removed by our protocol. An error of up to 2 μmol g^{-1} per measurement must be stated for our activity measurements.

In contrast, Cu-MOR prepared at pH > 6.0 could not be fully back-exchanged, indicating the presence of larger CuO particles on the surface, as shown by TEM. Activity tests revealed that, despite the significant Cu loading (Cu/Al 0.27), the catalyst showed a very poor productivity of 5 μmol g^{-1} which is less than 5% of the initial activity and close to the error of the measurement (see Table S2). This allows us to conclude, that large CuO particles are formed on samples exchanged at high pH. These particles are not active for the selective partial oxidation of methane to methanol.

S.3 Temperature programmed desorption of NH_3

Cu exchanged Na-MOR samples were first activated in vacuum for 2 h at 450 °C. The acid site concentration in a series of Na–MOR exchanged with Cu at pH 4 was determined by quantification of NH_3 desorbed after adsorption at 150 °C for 3 h and outgassing at 150°C and 260°C respectively for 2 h (Figure S4). Two distinct desorption peaks at 240 and 450 °C where observed after adsorption and outgassing at 150 °C. Outgassing at 260°C allowed quantification of the high temperature desorption peak. For both temperatures a linear correlation of Cu concentration and acid site concentration was found. The slope of the correlation after adsorption at 150°C was 2.03, whereas the slope after adsorption at 260°C was 0.90. The desorption peak at low temperature is due to weaker NH_3 adsorption on the Lewis acid sites, whereas the adsorption peak at 450 °C corresponds to strong adsorption of NH_3 on BAS. The offset of 210 μmol observed after adsorption and outgassing at 150 °C is due to NH_3 adsorbed on Lewis acidic extra-framework Al sites. Note that the slope of the correlation of BAS versus Cu concentration shows a value of 0.9 for both pyridine as well as NH_3 adsorption.

S.4 Determination of Na^+ concentration in side pockets

In a first step, the acid site concentration in the side pockets was determined by Na^+-exchange. Different concentrations of Na^+ were incorporated in the zeolite micropores via aqueous Na^+-exchange, as described in section 1.1 of supporting information. Infrared spectra of the so prepared Na-MOR materials with various Na^+ concentrations were compared to the spectra of pure H-MOR. Adsorption of n-hexane allowed selective perturbation of the main channel O-H-vibration (3612 cm^{-1}). Consequently, the O-H vibrations due to BAS in the side pockets were selectively examined by this technique. We observed, that the band at 3590 cm^{-1} decreased with increasing Na^+ loading and finally, the band disappeared when 750 μmol Na^+ ($Na/Al_F = 0.65$) were exchanged into the zeolite. Comparison of the infrared spectra before n-hexane adsorption revealed that the band attributed to main channel O-H vibrations remained unchanged up to a Na^+ concentration of 750 μmol g^{-1}. For higher Na^+ concentration also the main channel O-H-vibration decreased and finally disappeared when 1160 μmol g^{-1} Na^+ were exchanged into the zeolite. These experiments demonstrate the highly selective exchange of Na^+ into the 8-MR side pockets of MOR and at the same time allows us to quantify the BAS concentration in the side pockets.

Na^+ concentration in the side pockets after Cu-exchange of a fully exchanged Na-MOR was calculated by subtracting the Na^+ concentration in the main channel from the total Na^+ concentration. The Na^+ concentration in the main channel was determined by the difference from the amount of BAS in the main channel of the parent H-MOR (420 μmol g^{-1}) and the determined concentration of main channel BAS remaining in each CuNa-MOR sample, derived from the O-H vibration at 3612 cm^{-1}. This calculation is based on the fact that Cu^{2+} does not exchange in the main channel (as shown here in Table S3 and also in ref 6) and therefore the decrease intensity in the O-H vibration at 3612 cm^{-1} is solely attributed to Na^+ exchange.

S.5 Additional Figures

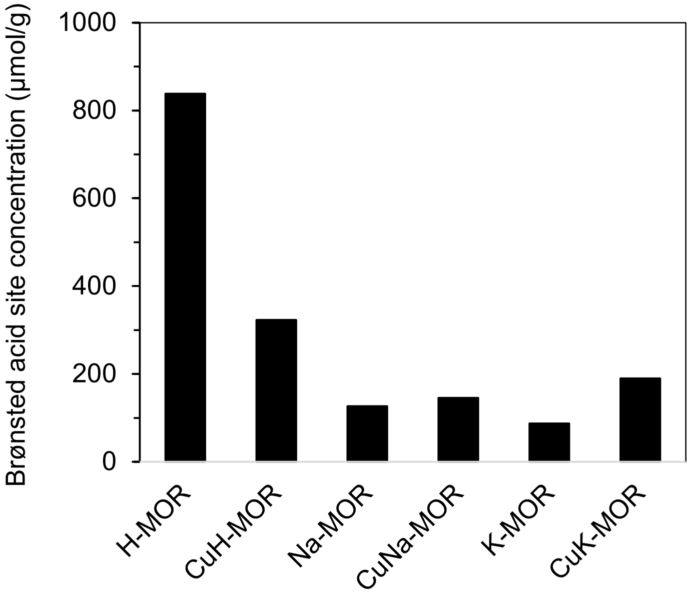

Figure S1. Impact of co-cations on Brønsted acidity. Brønsted acid site concentration of various MOR materials was quantified by the vibrational band of the pyridinium ion after adsorption of pyridine (1545 cm^{-1}). Cu exchange was performed at pH 5.7.

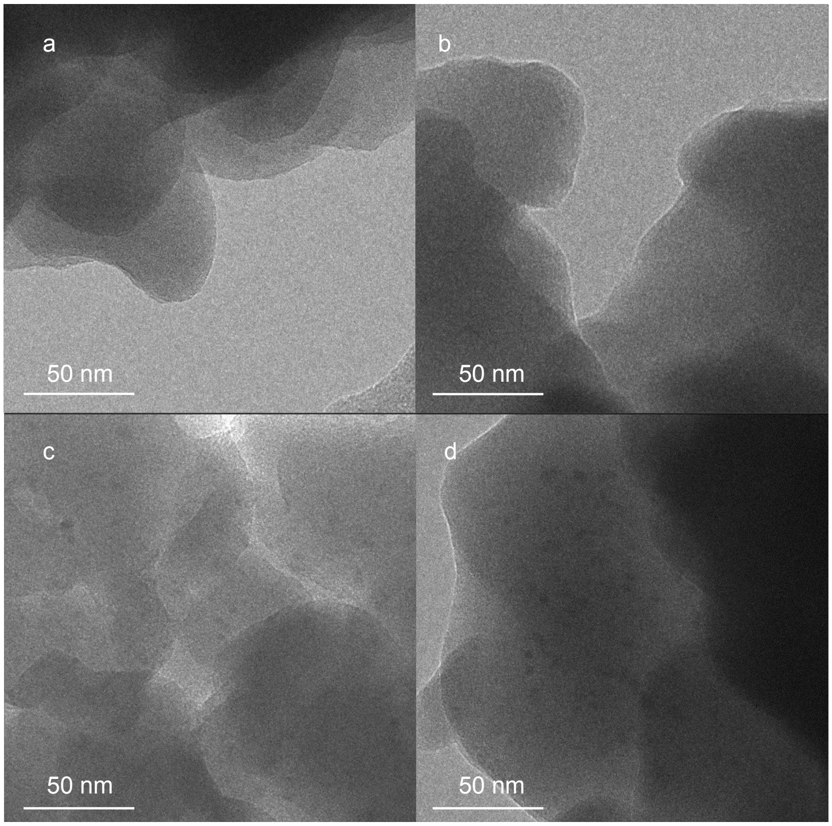

Figure S2. Transmission electron microscopy (TEM). Images of copper exchanged mordenites. a) CuH-MOR exchanged at pH 5.7 (Cu/Al 0.3), b) CuNa-MOR exchanged at pH 5.7 (Cu/Al 0.3), c) CuH-MOR exchanged at pH 6.6 (Cu/Al 0.6) and d) CuNa-MOR exchanged at pH 6.5 (Cu/Al 0.6).

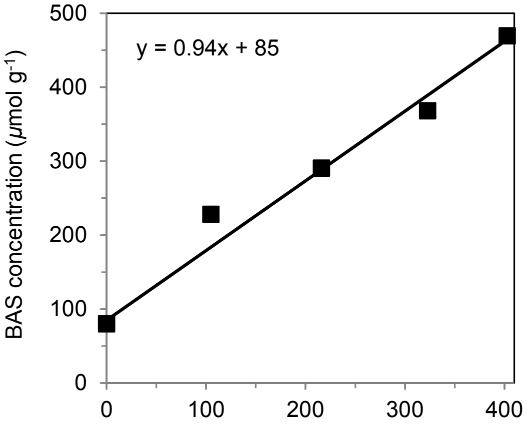

Figure S3. Brønsted acidity upon copper loading. Brønsted acid site concentration of CuNa-MOR quantified by the vibrational band of the pyridinium ion after adsorption of pyridine (1545 cm^{-1}) as a function of Cu loading. The series of CuNa-MOR was exchanged at pH 4.

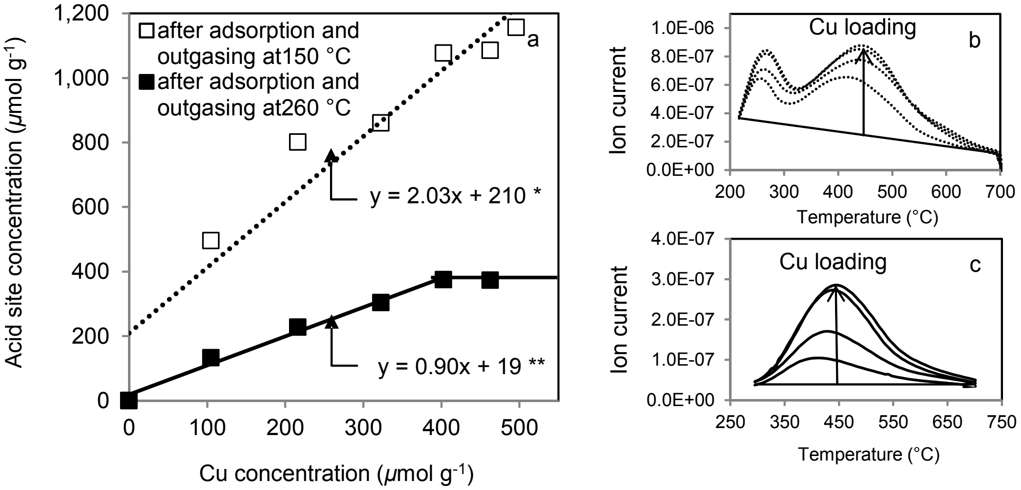

Figure S4. a) Acid site concentration determined by NH_3-TPD of CuNa-MOR as a function of Cu loading, b) NH_3-TPD curves after adsorption and outgassing at 150 ° and c) NH_3-TPD curves after adsorption and outgassing at 260 °C showing only one desorption peak attributed to NH_3 adsorbed on BAS. *The slope of 2.03 indicates formation of two acid sites per incorporated Cu. The offset of 210 μmol is attributed to NH_3 adsorbed on Lewis acidic extra-framework Al sites. **The slope of 0.90 indicates formation of one BAS per incorporated Cu.

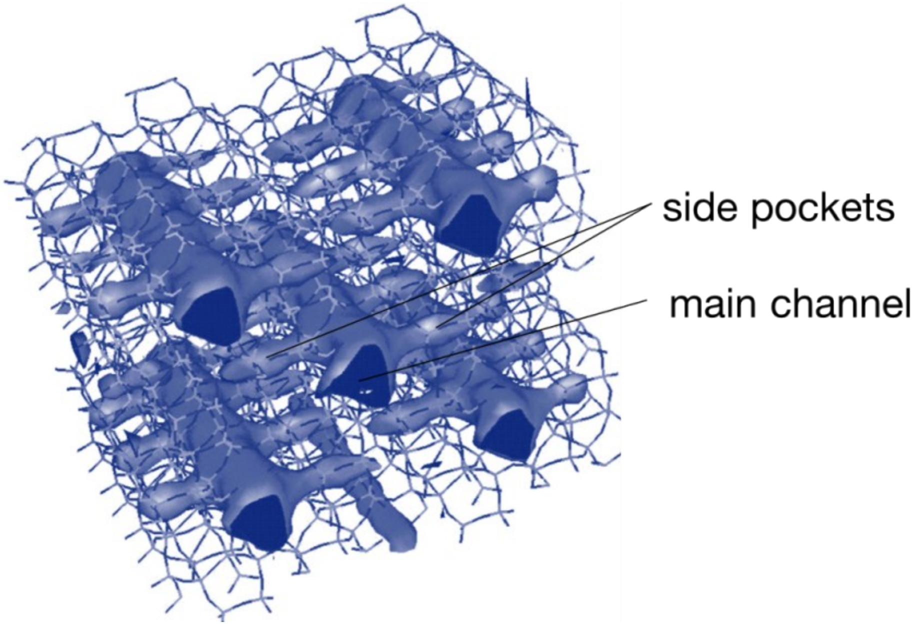

Figure S5. Mordenite topology. The MOR consists of a main channel composed of 12-MRs with perpendicular 8-MR side pockets. The side pockets are separated by a restriction of 2.6 x 5.7 Å, and their entrance (pore mouth) has an aperture of 3.9 x 5.7 Å. This diameter is substantially smaller than the aperture of the large 12MR straight channels (6.5 x 7.0 Å).

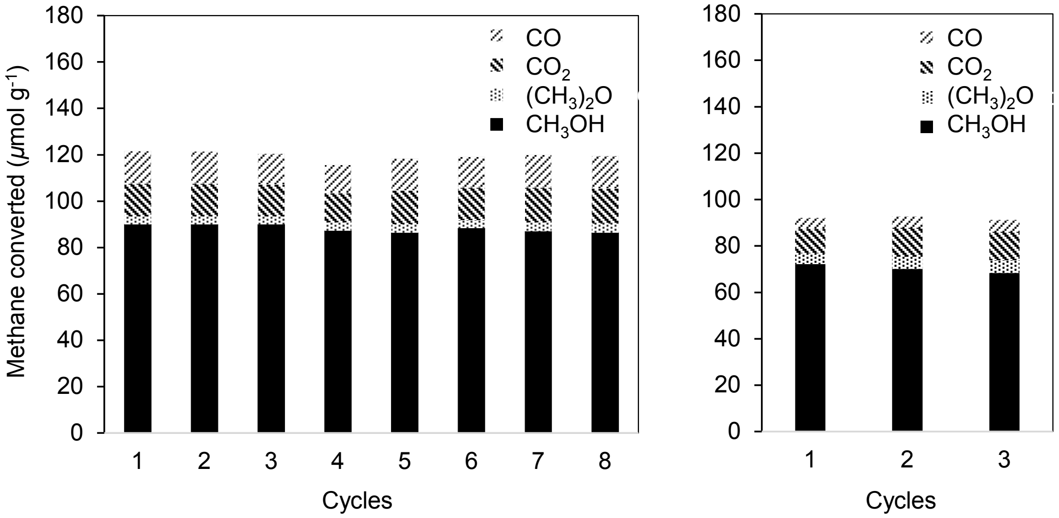

Figure S6. Catalytic stability of Cu-MOR. Stability test of a) Cu-MOR (Cu/Al 0.28) and b) CuNa-MOR (Cu/Al 0.32, Na/Al 0.25) for selective partial oxidation of methane to methanol. Recycling of the catalyst over 8 cycles with activation at 450 °C for 1h, methane loading at 200 °C for 30 min and steam treatment at 135 °C for 30 min in each cycle.

S.6 Additional Tables

Table S1. Elemental analysis of Cu-MOR with various co-cations

Sample	Cu loading [wt.%]	Co-cation loading [wt.%]	Cu/Al [mol mol^{-1}]	Co-cation/Al [mol mol^{-1}]
H-MOR	0.00	0.00	0.00	0.00
Cu-MOR	2.66	0.00	0.31	0.00
Na-MOR	0.00	2.45	0.00	0.85
CuNa-MOR	3.07	0.75	0.39	0.26
K-MOR	0.00	4.02	0.00	0.76
CuK-MOR	2.21	2.29	0.27	0.46
Mg-MOR	0.00	1.23	0.00	0.40
CuMg-MOR	2.45	0.63	0.29	0.19
Ca-MOR	0.0	2.14	0.00	0.41
CuCa-MOR	1.52	1.74	0.19	0.34

Table S2. Comparison of copper loading and activity of Cu-MORs prepared at various pH before and after back-exchange

Initial preparation				Back-exchange after calcination[a]	
sample	pH during Cu-exchange	Cu/Al [mol mol^{-1}]	Methane converted [μmol g^{-1}]	Cu/Al [mol mol^{-1}]	Methane converted [μmol g^{-1}]
CuH-MOR	4.4	0.21	99	0.02	2
CuNa-MOR	5.0	0.36	99	0.03	2
CuH-MOR	5.7	0.31	151	0.04	6
CuNa-MOR	6.5	0.61	115	0.27	5

[a] Samples were calcined under O_2 flow at 500 °C for 2 h and back-exchanged with 0.5 M $NaNO_3$ solution at 65 °C for 24 h.

Table S3. Acidity of CuH-MOR. Quantification of acid sites for a series of Cu-MOR[a] (Si/Al=11, Cu/Al ≤0.4)

Cu conc. [μmol g^{-1}]	BAS $_{\text{main channel}}$ [b] [μmol g^{-1}]	BAS $_{\text{SP bottom}}$ [c] [μmol g^{-1}]	BAS $_{\text{SP pore mouth}}$ [d] [μmol g^{-1}]	Total BAS [μmol g^{-1}]
0	400	310	380	1,090
100	430	270	330	1030
160	420	270	290	980
290	410	320	160	890
440	440	370	20	830

a) Total concentration of BAS in H-MOR (Si/Al=11) was determined by Na^+-exchange. For Cu-exchanged MOR the normalized integral of the O-H vibration of BAS was used for deconvolution and quantification.
b) Obtained by quantification of the band at 3,612 cm^{-1} (after deconvolution of the band at 3,605 cm^{-1} into 3,612, 3,590 and 3,500 cm^{-1}, see Supplementary Fig. 2).
c) Calculated by the difference of BAS concentration determined by a) and BAS concentration determined by pyridine.
d) Calculated by the difference between BAS concentration quantified after n-hexane adsorption (band at 3,590 cm^{-1}) and BAS concentration in the SP bottom (c); an offset of 70 μmol/g due to dealumination during Cu exchange was subtracted for H-MOR.

Table S4. Elemental analysis and acid site distribution in Cu exchanged mordenites.

Na [μmol g^{-1}]	Cu [μmol g^{-1}]	BAS$_{total}$ [μmol g^{-1}]	BAS$_{main\ channel}$ [a] [μmol g^{-1}]	BAS$_{side\ pockets}$ [b] [μmol g^{-1}]
0	419	800	420	380
307	384	385	358	27
319	414	303	282	21
948	102	240	240	0
421	401	469	384	85
718	216	291	291	0
618	266	268	268	0

a) Obtained by quantification of the band at 3,612 cm^{-1} (after deconvolution of the band at 3,610 cm^{-1} into 3,612, 3,590 and 3,500 cm^{-1}).

b) Obtained by quantification of the band at 3,590 cm^{-1} (after deconvolution of the band at 3,610 cm^{-1} into 3,612, 3,590 and 3,500 cm^{-1}).

Table S5. BET analysis of Cu exchanged mordenites.

Sample	Cu loading [wt.%]	Cu/Al [mol mol^{-1}]	BET surface area [m^2 g^{-1}]	$V_{micropore}$ [cm^3 g^{-1}]
H-MOR	0.0	0.00	534	0.20
Cu-MOR	1.0	0.12	499	0.18
Cu-MOR	2.9	0.34	501	0.19
Cu-MOR	5.2	0.62	422	0.16
Na-MOR	0.0	0.00	484	0.23
CuNa-MOR	3.1	0.39	430	0.21
CuNa-MOR	3.8	0.49	409	0.20
CuNa-MOR	5.0	0.61	371	0.17